



Published in final edited form as:

Cancer Discov. 2015 March ; 5(3): 316–331. doi:10.1158/2159-8290.CD-14-0736.

JAK-STAT Pathway Activation in Malignant and Non-Malignant Cells Contributes to MPN Pathogenesis and Therapeutic Response

Maria Kleppe^{1,*}, Minsuk Kwak^{2,*}, Priya Koppikar¹, Markus Riester³, Matthew Keller¹, Lennart Bastian¹, Todd Hricik¹, Neha Bhagwat^{1,4}, Anna Sophia McKenney^{1,4,5}, Efthymia Papalexi¹, Omar Abdel-Wahab^{1,6}, Raajit Rampal^{1,6}, Sachie Marubayashi¹, Jonathan J. Chen², Vincent Romanet⁷, Jordan S. Fridman⁸, Jacqueline Bromberg⁹, Julie Teruya-Feldstein¹⁰, Masato Murakami⁷, Thomas Radimerski⁷, Franziska Michor³, Rong Fan^{2,9,11,12}, and Ross L. Levine^{1,4,6,12}

¹Human Oncology and Pathogenesis Program, Memorial Sloan-Kettering Cancer Center, New York, New York, USA ²Department of Biomedical Engineering, Yale University, New Haven, Connecticut, USA ³Department of Biostatistics and Computational Biology, Dana-Farber Cancer Institute, and Department of Biostatistics, Harvard School of Public Health, Boston, Massachusetts, USA ⁴Gerstner Sloan-Kettering Graduate School of Biomedical Sciences, New York, New York, USA ⁵Weill Cornell/Rockefeller/Sloan-Kettering Tri-Institutional MD-PhD Program, New York, New York, USA ⁶Leukemia Service, Department of Medicine, Memorial Sloan-Kettering Cancer Center, New York, New York, USA ⁷Disease Area Oncology, Novartis Institutes for BioMedical Research, Basel, Switzerland ⁸Incyte Corporation, Wilmington, Delaware, US ⁹Breast Cancer Service, Department of Medicine, Memorial Sloan-Kettering Cancer Center, New York, New York, USA ¹⁰Department of Pathology, Memorial Sloan-Kettering Cancer Center, New York, New York, USA ¹¹Yale Comprehensive Cancer Center, New Haven, CT

Abstract

The identification of JAK2/MPL mutations in patients with myeloproliferative neoplasms (MPN) led to the clinical development of JAK kinase inhibitors, including ruxolitinib. Ruxolitinib reduces splenomegaly and systemic symptoms in myelofibrosis (MF) and improves overall survival; however the mechanism by which JAK inhibitors achieve efficacy has not been delineated. MPN

¹²To whom correspondence can be addressed: Rong Fan, Department of Biomedical Engineering, 55 Prospect Street, New Haven, CT 06520, rong.fan@yale.edu Ross L. Levine, Human Oncology and Pathogenesis Program, Leukemia Service, Department of Medicine, Memorial Sloan Kettering Cancer Center, 1275 York Avenue, Box 20, New York, NY 10065, leviner@mskcc.org.

*These authors contributed equally to this work

Author contributions

MKleppe and RLL conceived the project. MKleppe, MK, RF, and RLL designed experiments. MKleppe, MK, PK, MK, LB, EP, ASM, OAW, SM, JTF, RR, JJC, and MM performed experiments. MKleppe, MK, PK, MR, LB, TH, OAW, VR, RR, and MM analyzed data. JSF and JB provided reagents. MKleppe and RLL wrote the manuscript with input from MK, RF, PK, MR, OAW and FM.

Conflict of interest disclosure statement: TR, MM, MR, and VR are employees of Novartis Institutes for BioMedical Research. PK is currently an employee of Amgen and JSF was an employee of Incyte Corporation. RLL received grant support from Novartis for this study.

patients present with increased levels of circulating pro-inflammatory cytokines, which are mitigated by JAK inhibitor therapy. We sought to elucidate mechanisms by which JAK inhibitors attenuate cytokine-mediated pathophysiology. Single cell profiling demonstrated that hematopoietic cells from MF models and patient samples aberrantly secrete inflammatory cytokines. Pan-hematopoietic *Stat3* deletion reduced disease severity and attenuated cytokine secretion, with similar efficacy as observed with ruxolitinib therapy. By contrast, *Stat3* deletion restricted to MPN cells did not reduce disease severity or cytokine production. Consistent with these observations, we found that malignant and non-malignant cells aberrantly secrete cytokines and JAK inhibition reduces cytokine production from both populations.

Keywords

JAK2; MPN; cytokine signaling

Introduction

Myeloproliferative neoplasms are clonal hematopoietic disorders characterized by proliferation of one or more myeloid lineages (1). MPN patients develop progressive splenomegaly, thrombosis, bleeding, and/or infection. MPN patients are also at cumulative risk to develop progressive bone marrow failure and/or transform to acute myeloid leukemia (AML), conditions which are associated with dismal clinical outcome (2). The discovery of cytokine-independent colony formation of MPN progenitors suggested that constitutive cytokine signaling contributes to MPN pathogenesis (3). The observation of somatic activating *JAK2V617F* mutations in patients with polycythemia vera (PV), essential thrombocythemia (ET), and primary myelofibrosis (PMF) provided the first insight into the molecular basis of MPN (4–7). Subsequent studies identified somatic JAK-STAT pathway mutations in *JAK2V617F*-negative MPN, most commonly in the *CALR* gene (8, 9) and the thrombopoietin receptor (*MPLW515L*) (10). These data underscore the central importance of genetic alterations in the JAK-STAT signaling pathway in MPN pathogenesis.

The discovery of *JAK2/MPL* mutations in the majority of MPN patients provided the rationale for the clinical development of JAK kinase inhibitors for MPN patients and subsequently for other malignancies. Clinical studies with JAK kinase inhibitors have shown that these agents improve splenomegaly, systemic symptoms, and overall survival (11). Based on these data, ruxolitinib, a JAK1/JAK2 kinase inhibitor, was approved for MF patients and several other JAK inhibitors are in late phase clinical trials. Although JAK inhibitors offer substantial clinical benefit to MPN patients, the mechanisms by which these agents achieve clinical efficacy have not been fully delineated. MPN patients have significantly elevated circulating levels of pro-inflammatory cytokines, and increased circulating cytokine levels are associated with adverse survival in MF (12). It has been hypothesized that the cytokine-driven inflammatory state in MPN contributes to the constitutional symptoms, bone marrow fibrosis, extramedullary hematopoiesis and disease progression characteristic of these myeloid malignancies. JAK inhibitor therapy with ruxolitinib is associated with a reduction in the level of proinflammatory cytokines (13); however, the role of aberrant cytokine production in MF pathogenesis and in the response to

JAK inhibitors remains to be delineated. We therefore sought to elucidate the role of aberrant cytokine production in MPN pathogenesis and in the response to JAK kinase inhibitors. We employed a novel microfluidic single-cell profiling technique to examine the cytokine secretion profiles of MF cells on a single cell level and show that a significantly greater degree of multifunctionality and heterogeneity in cytokine production is a characteristic feature of MF cells. Moreover, we show that JAK-STAT signaling in non-mutant hematopoietic cells contributes to MPN pathogenesis and that inhibition of JAK-STAT signaling in both mutant and non-mutant cells is required to reduce inflammatory signaling and to achieve clinical benefit in MPNs.

Results

Pro-inflammatory cytokines are elevated in MF mice and reversed with JAK1/2 inhibitor treatment

In order to identify cytokines that are altered in MF, we measured the serum levels of 32 cytokines in the MPLW515L bone marrow transplant MF model (14) using multiplex bead-based Luminex technology. We identified a set of inflammatory cytokines, including Il6, Cxcl9, and Ccl2, which are elevated in the serum of MPLW515L-diseased mice (Fig. 1A), similar to the alterations in circulating cytokines observed in MF patients (12, 15). Ruxolitinib treatment (90mg/kg, BID) normalized cytokine levels, consistent with the effects seen with chronic JAK inhibition in MPN patients (Fig. 1A and Supplementary Fig. S1) (15). Circulating cytokine levels were also elevated in myelofibrotic (6-month old) *Jak2V617F;Vav-Cre* knock-in mice (16) (Fig. 1B), and ruxolitinib treatment (60mg/kg, BID) normalized cytokine levels in mice transplanted with *Jak2V617F*-mutant cells (Fig. 1C). Short-term ruxolitinib treatment (3 doses, 90mg/kg, BID) reduced cytokine production to a similar extent to that observed with 14 days of ruxolitinib treatment (90mg/kg, BID) (Fig. 1D), consistent with the rapid improvements in symptoms and splenomegaly seen with JAK inhibitor therapy (15) and with a direct effect of JAK kinase inhibition on cytokine secretion. The majority of cytokines (8 out of 10) were also increased in the bone marrow (BM) supernatant (Fig. 1E) of MPLW515L-diseased mice, suggesting that aberrant cytokine production in MF is, at least in part, derived from BM cells.

Bone marrow MF cells feature aberrant cytokine secretion profiles

In order to evaluate whether BM cells are the source of aberrant cytokine production in MF, we optimized a microchip system that allowed us to perform multiplexed measurements of up to 15 secretory cytokines from primary murine and human BM cells at single cell resolution (17–19) (Fig. 2A). Hierarchical cluster analysis of the single cell secretomic profiles delineated multiple distinct populations that displayed heterogeneous secretion signatures and revealed marked differences between MF and control BM cells (Fig. 2A). We observed a significant increase in the fraction of cytokine-secreting cells and in the extent of cytokine secretion per single MF cells (Fig. 2B). These data suggest the increased cytokine production in MF results from increased per-cell cytokine secretion and from an increase in the fraction of cytokine-secreting cells (Fig. 2C). The proportion of cells secreting at least one cytokine was significantly higher in MF mice compared to control mice (64.2% versus 47.1%, $P < 0.001$, Fisher's exact test). The majority of cytokine-secreting control BM cells

(72.8%) secreted less than two cytokines, consistent with physiologic secretion of one cytokine per cell. By contrast, we found that BM cells from MF mice were composed of a significantly elevated frequency of multifunctional cells that co-secrete multiple cytokines: 41.7% of cells from MF mice secreted two or more cytokines and 14.9% of cells secrete 4 or more cytokines compared to 0.9% in control mice (Fig. 2D).

In order to determine which cytokines were most frequently co-secreted by MF cells, we calculated a mutual exclusivity p -value for each pair of secreted cytokines (Fig. 2E). Ccl3, Ccl4, and Tnfa were commonly co-secreted in MF cells, and secretion of these cytokines was inversely correlated with the secretion of other cytokines (Fig. 2F). We observed co-secretion of all other cytokine combinations (Il6, Il12, Il10, Ccl2, Ccl5, Cxcl9, and Cxcl1) in MF cells, consistent with the presence of at least two distinct populations of cytokine-secreting cells in MF. In line with these observations, principal component analysis (PCA) demonstrated that a large proportion of normal BM cells did not secrete any protein and other smaller subsets with distinct secretion patterns produced only one or two cytokines, most notably, Ccl3 and Ccl4 (Fig. 2G and Supplementary Fig. S2). In contrast, PCA maps of MF BM cells showed multiple, large populations with heterogeneous secretion signatures. We then used the Simpson diversity index to quantify the extent of heterogeneity in cytokine secretion, and found that this index increased significantly from 0.68 in normal cells to 0.85 in MF cells ($P < 0.001$), consistent with a marked increase in the heterogeneity of single cell cytokine secretion in MF.

Mature myeloid and progenitor cells contribute to aberrant cytokine levels *in vivo*

We next sought to define which hematopoietic compartments contribute to aberrant cytokine secretion in MF. We used the single-cell platform to profile mature myeloid cells (CD11b/Gr1 double-positive) and megakaryocyte/erythroid progenitor (MEP) cells from MF and control mice. Similar to unfractionated BM cells, GFP-positive MF myeloid cells and MEP cells had an increase in the fraction of cytokine-secreting cells and increased cytokine secretion per cell (Supplementary Fig. S3). PCA analysis showed that each population had distinct cytokine secretion profiles (Fig. 3A). Il6 and Il10 were mainly secreted by MEPs, and mature myeloid cells were the main source of Tnfa and Ccl3 (Fig. 3B, Supplementary Fig. S3). These data indicate that different cell types have distinct cytokine secretion profiles and potentially distinct roles in MF pathogenesis.

Aberrant single-cell cytokine secretion in primary MF cells

We next performed single cell profiling of circulating granulocytes from MF patients and healthy individuals (Supplementary Table 1). The average secretion level of different cytokines was significantly elevated in MF cells, resulting from both an increase in the fraction of cells secreting specific cytokines and the secretion level of individual cytokines per cell (Fig. 3C and 3D). Six out of eight cytokines (Il6, Il10, Il12, Tnfa, Ccl2, and Ccl5), which were aberrantly secreted in our murine MF model were also secreted at a much higher level by primary MF patient cells. We observed that IL8 was most highly secreted by MF granulocytes; previous studies have shown that increased serum IL8 levels are associated with adverse outcome in MF (12). Immunohistochemical analysis confirmed increased IL8 expression in MF BM sections while control BM cells showed only weak expression of IL8

(Supplementary Fig. S4). The proportion of cells secreting at least one cytokine was significantly increased in human MF cells compared to control cells (41.4% versus 14.6%, $P < 0.001$, Fisher's exact test) (Fig. 3E) demonstrating similar patterns of cytokine secretion in MF patients and murine models. Altogether, our single cell profiling studies highlight the striking heterogeneity and multifunctionality in cytokine secretion profile in MF.

Deletion of *Il6* from the mouse system shows only minor effects on MPLW515L-driven disease

Previous studies of cytokine signaling in cancer have largely focused on *Il6* as a mediator of inflammation in leukemia and other malignancies (20). Given that we found a significant increase in *Il6* secretion in both MPN models and MF patient cells, we first investigated the effects of *Il6* deletion on MPLW515L-induced MF *in vivo*. We assessed the specific role of *Il6* in MF *in vivo* by transplanting *Il6*-deficient MF cells into *Il6*-deficient recipients. *Il6* deletion led to a modest reduction in white blood cell count, but did not reduce spleen weight or the extent of myeloproliferation *in vivo* (Supplementary Fig. S5A and B). No significant differences were observed in the proportion of CD11b/Gr-1 double positive cells in the target organs (Supplementary Fig. 5C and D). Consistent with these data, we found that the serum levels of other pro-inflammatory cytokines remained elevated in *Il6*-deficient MF mice, and we observed compensatory increases in *Il4* and *Il5* serum levels in the absence of *IL6* production (Supplementary Fig. 5E and F). While the specific role of other cytokines in MF requires further investigation, these data suggest that inflammatory signaling in MPN is driven by multiple cytokines, and that inhibiting secretion or signaling of an individual cytokine cannot attenuate the cytokine-signaling loop contributing to MPN pathogenesis.

Deletion of *Stat3* reduces cytokine production and ameliorates MF *in vivo*

We next aimed to investigate whether there are specific signaling pathways driving cytokine production *in vivo* in MF. First, in order to better characterize oncogenic signaling pathways activated by *JAK2/MPL* alleles *in vitro* and identify potential signaling effectors, we generated isogenic cell lines expressing the most common *JAK2* and *MPL* mutations observed in MPN patients. Notably, Ba/F3 cells expressing *MPLW515L* or *MPLW515L-JAK2V617F* showed evidence of constitutive *Stat3* activation (Supplementary Fig. S6). We also observed increased *Stat3* phosphorylation in splenocytes from MPLW515L-diseased mice and in the BM of primary MF patients (Supplementary Fig. S7). *JAK* inhibitor therapy reduced *Stat3* phosphorylation *in vivo* (Fig. 4A).

Previous studies have shown that *STAT3* signaling contributes to cytokine production in different malignant and inflammatory contexts (21); however the role of *STAT3* signaling in MPN inflammatory signaling and pathogenesis has not yet been elucidated. We thus performed MPLW515L bone marrow transplantations using hematopoietic-specific conditional *Stat3* knockout mice or respective littermate controls as donors (Supplementary Fig. S8). *Stat3* deletion improved survival, reduced disease severity, and reduced cytokine-mediated inflammation, similar to the effects observed with ruxolitinib therapy. *Stat3* deletion resulted in lower white blood counts, lower spleen weights, and a reduced degree of reticulin fibrosis (Fig. 4B–F and Supplementary Fig. S6), and decreased the proportion of

MEP cells in spleen and BM (Fig. 4G). Similar effects of *Stat3* deletion were seen with *Mx-Cre* and *Vav-Cre*, and with somatic deletion of *Stat3* after BM transplantation (Supplementary Fig. S9). Most importantly, hematopoietic specific *Stat3* deletion normalized circulating cytokine levels (Fig. 4H), with similar reductions in cytokine levels as with ruxolitinib therapy. These data demonstrate that *Stat3* activation is required for cytokine production in MF, and *Stat3* deletion phenocopies the effects of ruxolitinib on cytokine production and on disease sequelae *in vivo*.

Mutant-specific *Stat3* deletion does not reduce inflammatory signaling or myelofibrosis *in vivo*

It is currently not known if JAK inhibitors achieve clinical benefit solely from target inhibition in MPN cells, or if JAK-STAT inhibition in non-malignant cells contributes to therapeutic efficacy. We therefore examined if restricting *Stat3* deletion to mutant hematopoietic cells would result in similar effects as pan-hematopoietic *Stat3* deletion. We transplanted lethally irradiated CD45.1-positive recipient mice with MPLW515L-positive, *Stat3*-deleted BM (CD45.2-positive) along with *Stat3* wild-type support marrow (CD45.1-positive) (Fig. 5A and B). In contrast to the significant effects seen with complete hematopoietic *Stat3* deletion, MPN-specific *Stat3* deletion did not reduce disease severity (Fig. 5C and D, Supplementary Fig. S10). Consistent with these data, MPN-specific *Stat3* deletion did not significantly attenuate cytokine production, in contrast to the effects observed with pan-hematopoietic *Stat3* deletion (Fig. 5E). These data are consistent with a requirement for STAT3 signaling in both malignant and non-malignant hematopoietic cells in MF.

Cytokine production in MF originates in malignant and non-malignant hematopoietic cells

The genetic studies described above suggested that aberrant cytokine production in MF emanates from malignant and non-malignant hematopoietic cells. We therefore analyzed cytokine mRNA expression in sorted MPLW515L-mutant (GFP-positive) and wild-type (GFP-negative) BM cells using NanoString technology. We found that MPLW515L-mutant MF cells express high mRNA levels of a subset of inflammatory cytokines, including Il6, consistent with tumor-derived cytokine production (Fig. 6A). By contrast, we found that some cytokines, including Ccl2 and Tnfa, were derived from both GFP-positive and GFP-negative populations, and other cytokines, including Il12 and Cxcl9, were largely derived from non-mutant cells (Fig. 6A).

We then performed single cell analysis of sorted mutant and wild-type subpopulations to further delineate the contribution of malignant and non-malignant cells to cytokine production. Single cell analysis of lineage-positive (mature) and lineage-negative (hematopoietic stem/progenitor, HSPC) cells revealed that GFP-positive and GFP-negative cells from mature and HSPC compartments aberrantly secrete cytokines in MF (Fig. 6B and C). We observed an increase in cytokine secretion and in the degree of single-cell cytokine secretion heterogeneity in both GFP-positive and GFP-negative cells from stem/progenitor and differentiated cells compared to control BM cells (Supplementary Fig. S11). MPLW515L-mutant HSPCs were the largest source of Il6, whereas non-mutant mature cells were the primary source of Cxcl9 (Fig. 6B). Mutant and wild-type cells both secreted Tnfa,

Il10, and Ccl2 consistent with production by multiple populations (Fig. 6C). We observed an increase in total cytokine production and an increase in the proportion of cells which secreted multiple cytokines in GFP-positive/negative mature and GFP-positive HSPC from MF mice (Fig. 6D, Supplementary Fig. S11 and S12). Importantly, ruxolitinib treatment normalized cytokine expression from GFP-positive and GFP-negative cell populations (Fig. 6E), demonstrating that JAK inhibition reduces cytokine production from both tumor and non-tumor populations *in vivo*.

We next sought to extend our findings to JAK2V617F-mutant MPN. We transplanted whole bone marrow of *Jak2V617F;Vav-Cre* knock-in mice (CD45.2) with CD45.1 wild-type support marrow into CD45.1 recipient mice (MPN mice). After all mice engrafted with *Jak2V617F*-positive disease, we performed single cell cytokine analysis on sorted CD45.2 and CD45.1 cells to elucidate cytokine secretion in mutant and non-mutant cells (Fig. 7A). As a control we transplanted wild-type CD45.2 bone marrow with CD45.1 support cells into CD45.1 recipient mice (control mice). Single-cell cytokine profiling revealed marked differences in cytokine secretion in bone marrow cells derived from MPN and control mice (Supplementary Fig. S13). Most importantly, this included aberrant cytokine production in CD45.2 mutant and CD45.1 non-mutant cells from MPN mice. We observed an increase in the fraction of cytokine-secreting cells and in the extent of cytokine secretion per single cell in mutant and non-mutant hematopoietic populations from JAK2-mutant MPN mice (Fig. 7B and C, Supplementary Fig. S14). The proportion of cells secreting at least one cytokine was significantly higher within the wild-type population (CD45.1) of MF mice compared to the CD45.1 population of control mice (47.1% vs. 27%, $P < 0.001$, Fisher's exact test) (Fig. 7D). Similarly, 65% of CD45.2-positive *Jak2V617F*-expressing cells from MF mice secreted at least one cytokine compared to only 28.5% of control CD45.2 cells ($P < 0.001$, Fisher's exact test). Further, *Jak2V617F*-negative CD45.1-positive and *Jak2V617F*-positive CD45.2-positive bone marrow cells from MF exhibits a marked increase in the proportion of multifunctional cells that co-secrete multiple cytokines (Fig. 7D). Quantification of the extent of heterogeneity using the Simpson diversity index showed that non-mutant CD45.1-positive and *Jak2V617F*-positive, CD45.2-positive cells of diseased mice featured a significant increase in the heterogeneity of single cell secretion (CD45.1: 0.64 vs. 0.43, CD45.2: 0.74 vs. 0.44). Consistent with these data and with our data in the MPLW515L model, ruxolitinib treatment normalized cytokine expression from CD45.1- and CD45.2-positive cell populations in the *Jak2V617F* knock-in transplantation model (Supplementary Fig. S15). We next sought to investigate whether mutant and non-mutant cells in PMF could contribute to aberrant cytokine secretion. We identified a patient with PMF with a *JAK2V617F* mutant allele burden of 38%, consistent with partial involvement of the hematopoietic compartment of *JAK2V617F*-mutant cells (Supplementary Table 2). Notably, in this patient we found that 59% of the hematopoietic cells secreted one or more cytokines from our measurement (Fig. 7E). Also the frequency of multifunctional cells secreting two or more cytokines was significantly elevated in the patient (Fig. 7F). The proportion of cytokine secreting cells was greater than expected based on *JAK2V617F* mutant allele burden, suggesting that in this patient, a subset of *JAK2V617F* wild-type have to contribute to cytokine production. Taken together, these data illustrate the heterogeneity of aberrant

cytokine secretion in MPN models and patients, and that aberrant inflammatory signaling from more than one population contributes to MPN pathogenesis and therapeutic response.

Discussion

Although MPNs present as chronic myeloid malignancies, the quality of life and overall survival of primary myelofibrosis (PMF) patients is more similar to advanced malignancies including metastatic epithelial tumors. Patients with PMF have markedly elevated levels of pro-inflammatory cytokines, which are thought to contribute to PMF-associated symptoms and sequelae (12, 15). Clinical data show that JAK inhibition reduces constitutional symptoms and splenomegaly in PMF and post-PV/ET myelofibrosis patients, concurrent with a reduction in circulating cytokine levels (15). Although the prognostic value of circulating cytokine levels in MF has been previously demonstrated (12), the mechanisms that govern aberrant cytokine production in MF and the source of aberrant cytokines in MF has not previously been demonstrated. Here we show that JAK-STAT activation in malignant and non-malignant cells contributes to MF pathogenesis, and that cytokine production by both populations is an important feature of MF.

In this study, we demonstrate that JAK1/2 inhibition leads to a rapid, potent reduction in serum cytokine levels, consistent with the rapid clinical benefits seen with JAK inhibitor therapy and demonstrating this is a direct effect of JAK kinase inhibition on cytokine production. Single cell cytokine analysis showed that hematopoietic cells from MF models and PMF patients aberrantly secrete a spectrum of inflammatory cytokines. We performed multiplex, highly sensitive measurements of cytokine secretion from over a thousand of captured, viable single cells. The results demonstrated that hematopoietic cells in MF show significant up-regulation of a spectrum of pro-inflammatory cytokines, elevation of cellular heterogeneity in cytokine secretion, and increased multifunctional cytokine production, which are not observed in normal hematopoietic cells. Our data on a specific lineage, myeloid, demonstrated that both mature and progenitor myeloid cells contribute to increased cytokine production, and more interestingly they show distinct cytokine profiles suggesting their different roles in MF pathogenesis. Future studies will delineate the role of additional cytokines in inflammatory signaling in MPN, and use single-cell profiling to analyze non-hematopoietic cell types and previously unexplored hematopoietic lineages such as lymphoid cells and purified stem cells in MPN models/patient samples and in other malignancies to determine if multifunctional cytokine secretion is observed in other malignant contexts.

Many studies have identified *JAK2* mutations in MPN patients and in other malignancies, and several known *JAK2* signaling mediators have been linked to MPN disease manifestation and progression (22–24); however, the role of *STAT3* signaling in MPN pathogenesis and in inflammatory signaling in myeloid malignancies has not been previously delineated. *STAT3* represents a key link between cancer and inflammation, and as such provides an ideal candidate signaling effector driving cytokine production *in vivo*. In this study, we demonstrate a critical role for *STAT3* in inflammatory cytokine production in MF. Pan-hematopoietic *Stat3* deletion improved survival, reduced disease severity, and reduced cytokine secretion, with similar efficacy as observed with ruxolitinib therapy. By

contrast, restricting loss of *Stat3* to the malignant clone did not reduce disease severity or cytokine production, demonstrating that STAT3 signaling must be inhibited in malignant and non-malignant cells to achieve clinical efficacy. Consistent with these findings, we discovered that malignant and non-malignant cells aberrantly secrete inflammatory cytokines and that JAK inhibition reduces cytokine production from both populations. Our results demonstrate that JAK-STAT3 mediated cytokine production from malignant and non-malignant cells contributes to MPN pathogenesis and that JAK inhibition in both populations is required for therapeutic efficacy. These data reveal an important, unexpected mechanism of action of JAK inhibition in MPN, such that the target must be inhibited in tumor and non-tumor cells to achieve clinical benefit.

Recent studies in MPN models and in other hematologic malignancies have shown that additional, non-hematopoietic populations can influence malignant transformation, including nestin-positive stromal cells, osteoblasts, and other cell types in the hematopoietic niche (25–27). The role of cytokine secretion from these additional populations, particularly at single cell resolution, has not been explored to date. We believe that single-cell cytokine profiling can be used to elucidate the specific role of different niche populations in normal and malignant hematopoiesis and to assess the impact of JAK inhibitor therapy on the non-hematopoietic microenvironment in model systems and in primary patient samples, which should be the subject of subsequent investigations into cytokine secretion in different malignant states.

Taken together, our data underscore the critical role of aberrant cytokine signaling mediated by STAT3 activation in MPN pathogenesis. Most importantly, our studies support the notion that JAK kinase inhibition in malignant and non-malignant cells is required to achieve clinical efficacy in MF. Recent data has suggested that ruxolitinib improves overall survival in pancreatic cancer patients with evidence of systemic inflammation. As such, inhibition of cytokine signaling in malignant and non-malignant cells might offer clinical benefit in other malignancies characterized by aberrant inflammatory signaling. We hypothesize that JAK inhibition may have a broader role in cancer therapy, and that this therapeutic approach may improve outcomes for patients with malignancies characterized by systemic inflammation.

Methods Summary

Patient material

Patient studies were conducted in accordance with the Declaration of Helsinki. Primary patient samples were collected from MF patients and control healthy donors under MSKCC IRB Protocol 09-141. Ficoll technique was applied to isolate granulocytes from the peripheral blood of MF patients and healthy control individuals. JAK2 allele burden for MF patients were calculated using targeted sequencing approaches (RainDance, MiSeq).

Reagents and transgenic mice

Ruxolitinib was provided by Incyte/Novartis and formulated for administration by oral gavage as previously described (28). Conditional *Stat3* knock-out, *Jak2V617F* knock-in, and germline *Il6* knock-out mice have been described previously (16, 29). Floxed mice were crossed to the interferon-responsive *Mx-Cre* and *Vav-Cre* deleter lines. Congenic mice

(CD45.1) used as recipients in transplant studies were purchased from Jackson Laboratories. Antibodies used for Western blotting included phosphorylated and total JAK2, STAT3, STAT5, and MAPK (Cell Signaling). Mutant (GFP-positive) and wild-type (GFP-negative) populations were separated by fluorescent-activated cell sorting (FACS) using green fluorescent protein (GFP) and/or specific cell surface marker: phycoerythrin (PE)-conjugated CD11b, allophycocyanin (APC)-conjugated Gr1, Ter119 (APC-CY7), CD71 (PE-CY7), PE-conjugated CD117, Pacific Blue (PacBlue)-conjugated CD16/CD32, phycoerythrin-Cy7 (PeCy7)-conjugated Sca-1, and APC-conjugated CD34. All plasmids used in this study have been previously described (30). Lineage-positive (LIN+) and lineage-negative (LIN-) subpopulations were separated using a panel of APC-CY7-conjugated antibodies that recognize all mature hematopoietic lineages (CD4, CD19, CD11b, Gr1, Ter119, CD3, B220, and NK1.1).

Bone marrow transplantation model

All animal experiments were performed in accordance with our Memorial Sloan Kettering Cancer Center Institutional Animal Care and Use Committee-approved animal protocol. Animal care was in strict compliance with institutional guidelines established by the Memorial Sloan-Kettering Cancer Center, the Guide for the Care and Use of Laboratory Animals (National Academy of Sciences 1996), and the Association for Assessment and Accreditation of Laboratory Animal Care International. MPLW515L bone marrow transplantation experiments were performed as described previously (14). Briefly, pre-stimulated c-kit enriched bone marrow cells were subjected to two rounds of co-sedimentation with viral supernatant containing MSCV-*hMPLW515L*-IRES-GFP or empty MSCV-IRES-GFP control vector. A total of 1×10^6 cells (~25–40% GFP-positive, MPL-expressing cells) were injected into the tail veins of lethally irradiated syngeneic mice. For secondary *Jak2V617F;Vav-Cre* bone marrow transplantations, 5×10^6 bone marrow cells harvested from sick *Jak2V617F* knock-in mice were injected into the tail veins of 8-week old syngeneic mice (16). Engrafted mice were monitored daily for signs of illness and nonlethal bleeds were performed bi-weekly to follow up disease progression. Mice showing signs of being moribund, more than 10% weight loss or palpable splenomegaly extending across the midline were sacrificed. Spleens were removed, weighed and single cell suspensions were prepared for subsequent cell staining and fractionation, Western blot analysis, or histopathological analysis. Peripheral blood chimerism was routinely determined 14 days post bone marrow transplantation. *Stat3* excision was confirmed by western blot and quantitative real-time PCR analysis on red cell lysed peripheral blood samples.

Inhibitor experiments

At first signs of disease, mice were randomized to begin 14 or 21 days of treatment with the JAK1/2 inhibitor ruxolitinib (90mg/kg (Balb/c, MPLW515L) or 60mg/kg (C57/B16, secondary *Jak2V617F* recipient mice), *p.o.*, BID) or vehicle followed by measurement of plasma cytokine levels. Mice were ranked based on baseline white blood cell count (WBC) and assigned to treatment groups to achieve congruent WBC profiles. Serum was collected four hours after last drug administration. For kinetic studies, mice assigned for short-term drug treatment received only three doses, which were administered simultaneously with the last doses of the long-term treatment arm.

Luminex technology

Luminex assays were carried out using the FlexMAP 3D multiplexing platform (Luminex xMAP system). Plasma levels of 32 cytokines were measured simultaneously using the Millipore Mouse Cytokine 32-plex kit. Serum samples were prepared following manufactures instructions. xPONENT (Luminex) and Milliplex Analyst Software (Millipore) was applied to convert mean fluorescent intensities (MFI) values into molecular concentrations by the use of a standard curve (5-parameter logistic fitting method).

Histopathological analysis

Femur and spleen samples were fixed in 4% paraformaldehyde overnight and then embedded in paraffin as previously described (31). Paraffin sections were cut on a rotary microtome (3 μ m, Mikrom International AG), spread in a 45°C water-bath, mounted on microscope slides (Thermo Scientific) and air-dried in an oven at 37°C overnight. After drying, tissue section slides were processed either automatically for H&E staining (COT20 stainer, Medite) or manually for reticulum staining with silver impregnation method kit (Bio-Optica). Slides were scanned with Scanscope XT slide scanner (Aperio). Pictures were taken at a 20x (H&E and reticulin) magnification by using Imascope viewer (Aperio). For the expression analysis of IL8 and phospho-STAT3, 5 μ m unstained sections from cases of bone marrow samples were stained on the Ventana Discovery XT (Tuscon, AZ) per manufacturer's instructions. The following antibodies were used: goat IL-8 antibody from R&D Systems (1:40 dilution), monoclonal rabbit anti-phospho-STAT3 antibody from Cell Signaling (1:50 dilution). Photomicrographs were taken using an Olympus BX41 with DP20 software.

Single-cell cytokine secretion assay

A high-density antibody barcode was created using a microchannel-guided flow patterning technique as previously described (17, 18). A polydimethylsiloxane microchip with 20 microfluidic channels for flow patterning was fabricated using a soft lithography technique. After the microchip was bonded with a poly-L-lysine glass slide, the capture antibody for each cytokine was injected into a microfluidic channel and flowed through the chip via air pressure (1.8 psi, 12 hours). Antibodies were then immobilized on the glass slide to form the antibody barcode. The sub-nanoliter microchamber array for single cell capture is a one-layer polydimethylsiloxane slab fabricated using a soft-lithography method and contains 7700 microchambers (17, 32). A single cell suspension of bone marrow cells was prepared in RPMI 1640 supplemented with 20% FBS, Ii3, Scf, and IL6 at a density of 400,000 cells/mL. After blocking with 3% BSA/PBS (2 hours), 200 μ L of the single cell suspension was pipetted onto the chip and allowed to settle (5 minutes). Normally ~25% of the microchambers contained single cells based on the Poisson distribution (17). The antibody barcode glass slide was then put on top of the microchambers. Assembled microchamber arrays were then imaged (Nikon Eclipse Ti) to determine number of cells in each microchamber by using a custom-made image-processing algorithm. After incubation (24h, 37°C in 5% CO₂), the cytokine signals from antibody barcode chips were developed via an immuno-sandwich ELISA assay. The slide was scanned with GenePix 4200A (Axon) microarray scanner to collect fluorescent signals. All fluorescent scanned images were

processed with GenePix software and excel macro to acquire average fluorescent signals from each microchamber for all bars in each antibody barcode set, and the fluorescent signals were matched with the number of cells. Single-cell data were gated based on the background signals to distinguish between cytokine-producers and non-producers. The data was further transformed and normalized to perform multi-dimensional data analysis as previously described (18, 33–35).

Data processing and analysis of single cell cytokine assays

For all single-cell secretomic analysis, our custom built algorithms in Excel, MATLAB, and R-packages were employed to process, analyze, and visualize the single-cell cytokine profiles. Briefly, the pre-determined cell numbers of the microchambers were matched with fluorescence intensity values for each measured proteins from corresponding microchambers. The background signals from all zero-cell (empty) microchambers were used to determine the gate in order to detect cytokine-producing cells and non-producers. The gating threshold was calculated by (average intensity of all empty microchambers for a given cytokine) + 2*(standard deviation of all empty microchambers for a given cytokine) (35). Any cells with fluorescence intensity of a specific cytokine below the gating threshold were considered non-producers, and their cytokine intensity values were converted to 0. Any cells with fluorescence intensity above the gating threshold were considered as cytokine-producers, and given the cytokine intensity value of (the measured fluorescence intensity – the average fluorescence intensity of all zero-cell microchambers for a given cytokine). The gated and background-subtracted cytokine intensity values were log-transformed. In order to eliminate variability in detection sensitivity and profile the secretion of all assayed proteins, each protein was normalized by the average intensity and the standard deviation. The number of all cells above the gates and the sum of fluorescence intensity of a given cytokine were measured to calculate the frequency of cytokine-producers and the average cytokine secretion per single cell. For the single-cell analysis of unsorted, whole bone marrow compartment, the data were processed without log transformation. By not conducting log transformation, which significantly suppresses the data range, we could distinguish smaller subsets with unique cytokine profiles from the more heterogeneous and larger unsorted bone marrow cell population. Our statistical analysis and graphical representations of the single-cell secretomic profiles are based on the methods routinely used to analyze large-scale high-dimensional datasets from numerous cell subsets (18, 33–35).

Principal component, mutual exclusivity, and statistical analysis

All analyses were performed in R. The PCA was performed utilizing the `prcomp` R function and visualized with the `ggplot2` package. The first two principal components explained 60.1% of the variance. PC3 and PC4 (cumulative proportion of variance 78%) were, similar to PC1 and PC2, mainly defined by secretion of *Tnfa*, *Ccl3*, *Ccl4*, *Cxcl1* and *Ccl5* (Supplementary Fig. 1a). Since PC3 to PC4 covered essentially the same cytokines as PC1 and PC2, we focused on the visualization of the first two PCs. PC5 (83%) was dominated by *Il10* secretion. We next tested whether two cytokines were less (mutual exclusivity) or more frequently co-secreted than expected by chance. To this end, we created for each pair of cytokines a 2×2 contingency table (secreted only in cytokine A; only in B; in both A and B; in neither A nor B) and obtained a p-value with Fisher's exact test. P-values were adjusted

for multiple testing using the Benjamini-Hochberg correction and a false discovery rate (FDR) < 0.05 was considered significant. FDRs were visualized in a heat map, with pairs of cytokines displaying significant co-secretion colored in red, and mutual exclusive pairs in light yellow. Pairs with co-secretion patterns not significantly different from randomly expected patterns were shown in grey. We further tested whether pairs of cytokines are more or less frequently co-secreted in MF mice compared to control mice. We again used a Fisher's exact test to obtain p-values for the corresponding 2x2 contingency table (number of co-secreted cells in MF, number of non-co-secreted cells in MF, number of co-secreted cells in control mice, number of non-co-secreted cells in control mice). Only cells with at least two secreted cytokines were considered in this mutual exclusivity analysis.

Statistical analysis

The Student's *t*-test was used to compare the mean of two groups. Normality tests were used to test the assumption of a normal distribution. Graphs represent mean values \pm s.e.m. Kaplan-Meier survival analysis and longrank test was used to compare survival outcomes between the two groups.

Supplementary Material

Refer to Web version on PubMed Central for supplementary material.

Acknowledgments

Grant support: This work was supported by the Dana-Farber Cancer Institute's Physical Sciences Oncology Center (U54CA143798-01) to RLL, RF, MR, and FM and by NCI 1R01CA151949-01 to RLL, NCI 1R01CA138234-01 to FM and RLL, and partly by NIDDK 1U01DK104331-01 to RF and RLL. MKleppe is a fellow of the Leukemia and Lymphoma Society and was previously supported by an EMBO Long-Term Fellowship. A.S.M. was supported by a Medical Scientist Training Program grant from the National Institute of General Medical Sciences of the National Institutes of Health under award number: T32GM007739 to the Weill Cornell/Rockefeller/Sloan-Kettering Tri-Institutional MD-PhD Program. RLL is a Leukemia and Lymphoma Society Scholar.

We thank members of the Levine and Fan laboratories, Neal Rosen, and Scott Armstrong for helpful comments and discussion. We thank Benjamin L. Ebert (Harvard Medical School) and Ann Mullally (Harvard Medical School) for providing *Jak2V617F* knock-in mice. We are grateful to the MSK Kravis Center for Molecular Oncology/Geoffrey Beene Core for their assistance with NanoString and targeted sequencing analysis and Irina Linkov (IHC Pathology Core) and Janine Pichardo for technical assistance with pathological experiments. We also acknowledge the support from the Yale Institute for Nanoscience and Quantum Engineering (YINQE) and the Yale Nanofabrication Center for allowing us to use their microfabrication facilities.

References

1. Tefferi A, Vardiman JW. Myelodysplastic syndromes. *N Engl J Med*. 2009; 361:1872–85. [PubMed: 19890130]
2. Tam CS, Nussenzeig RM, Popat U, Bueso-Ramos CE, Thomas DA, Cortes JA, et al. The natural history and treatment outcome of blast phase BCR-ABL- myeloproliferative neoplasms. *Blood*. 2008; 112:1628–37. [PubMed: 18566326]
3. Delhommeau F, Jeziorowska D, Marzac C, Casadevall N. Molecular aspects of myeloproliferative neoplasms. *Int J Hematol*. 2010; 91:165–73. [PubMed: 20186505]
4. Baxter EJ, Scott LM, Campbell PJ, East C, Fourouclas N, Swanton S, et al. Acquired mutation of the tyrosine kinase JAK2 in human myeloproliferative disorders. *Lancet*. 2005; 365:1054–61. [PubMed: 15781101]

5. Kralovics R, Passamonti F, Buser AS, Teo SS, Tiedt R, Passweg JR, et al. A gain-of-function mutation of JAK2 in myeloproliferative disorders. *The New England journal of medicine*. 2005; 352:1779–90. [PubMed: 15858187]
6. Levine RL, Wadleigh M, Cools J, Ebert BL, Wernig G, Huntly BJ, et al. Activating mutation in the tyrosine kinase JAK2 in polycythemia vera, essential thrombocythemia, and myeloid metaplasia with myelofibrosis. *Cancer Cell*. 2005; 7:387–97. [PubMed: 15837627]
7. James C, Ugo V, Le Couedic JP, Staerk J, Delhommeau F, Lacout C, et al. A unique clonal JAK2 mutation leading to constitutive signalling causes polycythaemia vera. *Nature*. 2005; 434:1144–8. [PubMed: 15793561]
8. Klampfl T, Gisslinger H, Harutyunyan AS, Nivarthi H, Rumi E, Milosevic JD, et al. Somatic mutations of calreticulin in myeloproliferative neoplasms. *N Engl J Med*. 2013; 369:2379–90. [PubMed: 24325356]
9. Nangalia J, Massie CE, Baxter EJ, Nice FL, Gundem G, Wedge DC, et al. Somatic CALR mutations in myeloproliferative neoplasms with nonmutated JAK2. *N Engl J Med*. 2013; 369:2391–405. [PubMed: 24325359]
10. Tefferi A. Molecular drug targets in myeloproliferative neoplasms: mutant ABL1, JAK2, MPL, KIT, PDGFRA, PDGFRB and FGFR1. *J Cell Mol Med*. 2009; 13:215–37. [PubMed: 19175693]
11. Quintas-Cardama A, Kantarjian H, Cortes J, Verstovsek S. Janus kinase inhibitors for the treatment of myeloproliferative neoplasias and beyond. *Nature reviews Drug discovery*. 2011; 10:127–40.
12. Tefferi A, Vaidya R, Caramazza D, Finke C, Lasho T, Pardanani A. Circulating interleukin (IL)-8, IL-2R, IL-12, and IL-15 levels are independently prognostic in primary myelofibrosis: a comprehensive cytokine profiling study. *J Clin Oncol*. 2011; 29:1356–63. [PubMed: 21300928]
13. Verstovsek S, Kantarjian H, Mesa RA, Pardanani AD, Cortes-Franco J, Thomas DA, et al. Safety and efficacy of INCB018424, a JAK1 and JAK2 inhibitor, in myelofibrosis. *The New England journal of medicine*. 2010; 363:1117–27. [PubMed: 20843246]
14. Pikman Y, Lee BH, Mercher T, McDowell E, Ebert BL, Gozo M, et al. MPLW515L is a novel somatic activating mutation in myelofibrosis with myeloid metaplasia. *PLoS Med*. 2006; 3:e270. [PubMed: 16834459]
15. Verstovsek S, Kantarjian H, Mesa RA, Pardanani AD, Cortes-Franco J, Thomas DA, et al. Safety and efficacy of INCB018424, a JAK1 and JAK2 inhibitor, in myelofibrosis. *N Engl J Med*. 2010; 363:1117–27. [PubMed: 20843246]
16. Mullally A, Lane SW, Ball B, Megerdichian C, Okabe R, Al-Shahrour F, et al. Physiological Jak2V617F expression causes a lethal myeloproliferative neoplasm with differential effects on hematopoietic stem and progenitor cells. *Cancer Cell*. 2010; 17:584–96. [PubMed: 20541703]
17. Lu Y, Chen JJ, Mu L, Xue Q, Wu Y, Wu PH, et al. High-throughput secretomic analysis of single cells to assess functional cellular heterogeneity. *Anal Chem*. 2013; 85:2548–56. [PubMed: 23339603]
18. Ma C, Fan R, Ahmad H, Shi Q, Comin-Anduix B, Chodon T, et al. A clinical microchip for evaluation of single immune cells reveals high functional heterogeneity in phenotypically similar T cells. *Nat Med*. 2011; 17:738–43. [PubMed: 21602800]
19. Fan R, Vermesh O, Srivastava A, Yen BK, Qin L, Ahmad H, et al. Integrated barcode chips for rapid, multiplexed analysis of proteins in microliter quantities of blood. *Nat Biotechnol*. 2008; 26:1373–8. [PubMed: 19029914]
20. Schepers K, Pietras EM, Reynaud D, Flach J, Binnewies M, Garg T, et al. Myeloproliferative neoplasia remodels the endosteal bone marrow niche into a self-reinforcing leukemic niche. *Cell Stem Cell*. 2013; 13:285–99. [PubMed: 23850243]
21. Yu H, Pardoll D, Jove R. STATs in cancer inflammation and immunity: a leading role for STAT3. *Nat Rev Cancer*. 2009; 9:798–809. [PubMed: 19851315]
22. Walz C, Ahmed W, Lazarides K, Betancur M, Patel N, Hennighausen L, et al. Essential role for Stat5a/b in myeloproliferative neoplasms induced by BCR-ABL1 and JAK2(V617F) in mice. *Blood*. 2012; 119:3550–60. [PubMed: 22234689]
23. Yan D, Hutchison RE, Mohi G. Critical requirement for Stat5 in a mouse model of polycythemia vera. *Blood*. 2012; 119:3539–49. [PubMed: 22144185]

24. Kleppe M, Levine RL. New pieces of a puzzle: the current biological picture of MPN. *Biochim Biophys Acta*. 2012; 1826:415–22. [PubMed: 22824378]
25. Arranz L, Sanchez-Aguilera A, Martin-Perez D, Isern J, Langa X, Tzankov A, et al. Neuropathy of haematopoietic stem cell niche is essential for myeloproliferative neoplasms. *Nature*. 2014; 512:78–81. [PubMed: 25043017]
26. Reynaud D, Pietras E, Barry-Holson K, Mir A, Binnewies M, Jeanne M, et al. IL-6 controls leukemic multipotent progenitor cell fate and contributes to chronic myelogenous leukemia development. *Cancer Cell*. 2011; 20:661–73. [PubMed: 22094259]
27. Hanoun M, Zhang D, Mizoguchi T, Pinho S, Pierce H, Kunisaki Y, et al. Acute myelogenous leukemia-induced sympathetic neuropathy promotes malignancy in an altered hematopoietic stem cell niche. *Cell Stem Cell*. 2014; 15:365–75. [PubMed: 25017722]
28. Quintas-Cardama A, Vaddi K, Liu P, Manshoury T, Li J, Scherle PA, et al. Preclinical characterization of the selective JAK1/2 inhibitor INCB018424: therapeutic implications for the treatment of myeloproliferative neoplasms. *Blood*. 2010; 115:3109–17. [PubMed: 20130243]
29. Takeda K, Kaisho T, Yoshida N, Takeda J, Kishimoto T, Akira S. Stat3 activation is responsible for IL-6-dependent T cell proliferation through preventing apoptosis: generation and characterization of T cell-specific Stat3-deficient mice. *J Immunol*. 1998; 161:4652–60. [PubMed: 9794394]
30. Wernig G, Gonneville JR, Crowley BJ, Rodrigues MS, Reddy MM, Hudon HE, et al. The Jak2V617F oncogene associated with myeloproliferative diseases requires a functional FERM domain for transformation and for expression of the Myc and Pim proto-oncogenes. *Blood*. 2008; 111:3751–9. [PubMed: 18216297]
31. Koppikar P, Abdel-Wahab O, Hedvat C, Marubayashi S, Patel J, Goel A, et al. Efficacy of the JAK2 inhibitor INCB16562 in a murine model of MPLW515L-induced thrombocytosis and myelofibrosis. *Blood*. 2010; 115:2919–27. [PubMed: 20154217]
32. Unger MA, Chou HP, Thorsen T, Scherer A, Quake SR. Monolithic microfabricated valves and pumps by multilayer soft lithography. *Science*. 2000; 288:113–6. [PubMed: 10753110]
33. Bodenmiller B, Zunder ER, Finck R, Chen TJ, Savig ES, Bruggner RV, et al. Multiplexed mass cytometry profiling of cellular states perturbed by small-molecule regulators. *Nat Biotechnol*. 2012; 30:858–67. [PubMed: 22902532]
34. Qiu P, Simonds EF, Bendall SC, Gibbs KD Jr, Bruggner RV, Linderman MD, et al. Extracting a cellular hierarchy from high-dimensional cytometry data with SPADE. *Nat Biotechnol*. 2011; 29:886–91. [PubMed: 21964415]
35. Zhao JL, Ma C, O'Connell RM, Mehta A, DiLoreto R, Heath JR, et al. Conversion of danger signals into cytokine signals by hematopoietic stem and progenitor cells for regulation of stress-induced hematopoiesis. *Cell Stem Cell*. 2014; 14:445–59. [PubMed: 24561084]

Significance

Our results demonstrate that JAK-STAT3 mediated cytokine production from malignant and non-malignant cells contributes to MPN pathogenesis and that JAK inhibition in both populations is required for therapeutic efficacy. These findings provide novel insight into the mechanisms by which JAK kinase inhibition achieve therapeutic efficacy in MPNs.

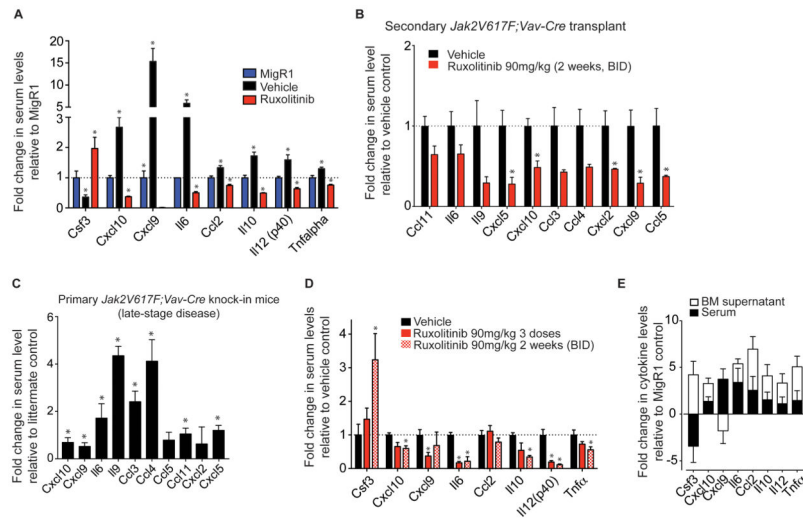


Figure 1. Pro-inflammatory cytokines are elevated in MF mice and normalized with JAK inhibition

A, Changes in cytokine levels in vehicle- and ruxolitinib-treated MPLW515L mice compared with MigR1 mice. $n=6$. $*P<.05$. **B**, Ruxolitinib (90mg/kg, twice a day) reduces cytokines in mice transplanted with *Jak2V617F;Vav-Cre*-positive cells. $n=4$. $*P<.05$. **C**, Log₂ fold changes in serum cytokine levels in primary *Jak2V617F* knock-in mice (late stage disease) compared to age-matched littermate controls are shown. Mean \pm SEM, $n=9$ in each group. **D**, Short-term treatment (3 doses, 90mg/kg, BID) with ruxolitinib efficiently reduces serum cytokine levels in MPLW515L diseased mice. Log₂ fold changes are displayed. $n=4$. $*P<.05$. **E**, Log₂-fold changes in serum and bone marrow supernatant in MPLW515L mice compared to MigR1 mice. Mean \pm s.e.m.

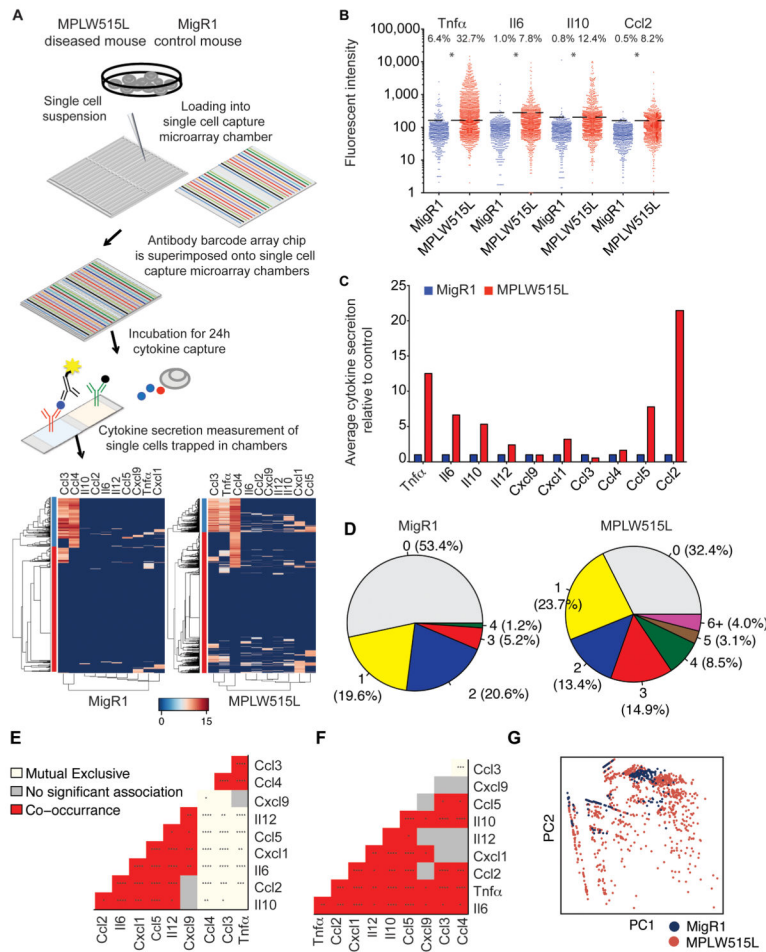


Figure 2. Bone marrow cells are potent cytokine producers

A, Schematic display of single cell cytokine secretion analysis workflow and hierarchical clustering of single cell data from MPLW515L and MigR1 whole bone marrow. Log₂-transformed values were used for cluster analysis. **B**, Normalized fluorescent intensity for different cytokines. Numbers on top show cytokine secretion frequency. Dotted lines indicate cytokine secretion threshold. **P* < .05. **C**, Total secretion levels (cytokine secretion fraction x average secretion intensity of cytokine secreting cells) of MPLW515L mice bone marrow (MPLW515L) relative to healthy control mice (MigR1) are shown. **D**, Pie charts depicting proportion of MigR1 and MPLW515L bone marrow cells secreting different numbers of cytokines (0–10). **E**, Mutual exclusivity analysis for MF cells. FDR: + < 0.05, ++ < 0.01, +++ < 0.001 and ++++ < 0.0001. Red/White without pluses is FDR < 0.1. **F**, Comparison between co-secretion patterns observed in MF and control cells. Colors visualize FDR. **G**, PCA of MPLW515L and MigR1 cytokine secretion. MPLW515L: *n*=2254 cells, MigR1 cells: *n*=608 cells.

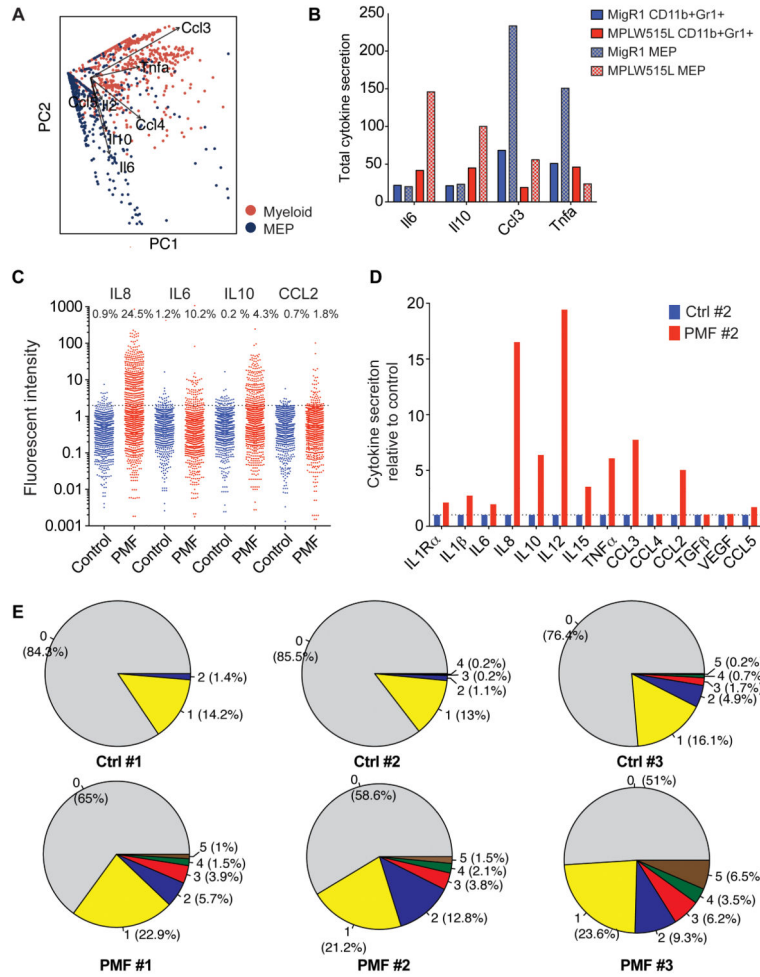


Figure 3. Pathologic secretion of multiple cytokines by MF cells

A, PCA analysis of single cell cytokine secretion data from MPLW515L-expressing MEP and myeloid cells identified two principal components, largely defined by production of IL6 and IL10 (PC1, MEP) Ccl3, and Tnfa (PC2, myeloid). **B**, Total secretion levels (*cytokine secretion fraction x average secretion intensity of cytokine secreting cells*) of sorted GFP-positive cells from MPLW515L mice bone marrow (MPLW515L) compared to control healthy mice (MigR1) are shown. **C**, Normalized fluorescent intensity for different cytokines. Numbers on top show cytokine secretion frequency. Dotted lines indicate cytokine secretion threshold. **D**, Total secretion levels of human PMF granulocytes (PMF #2) relative to control cells (Ctrl #2) are shown. PMF #2: $n=1318$ analyzed cells, control granulocytes: $n=976$ analyzed cells. **E**, Pie charts depicting percentage of human PMF granulocytes (PMF) and control cells secreting different numbers of cytokines. Numbers in brackets represent the percentage of cells secreting a given number of cytokines.

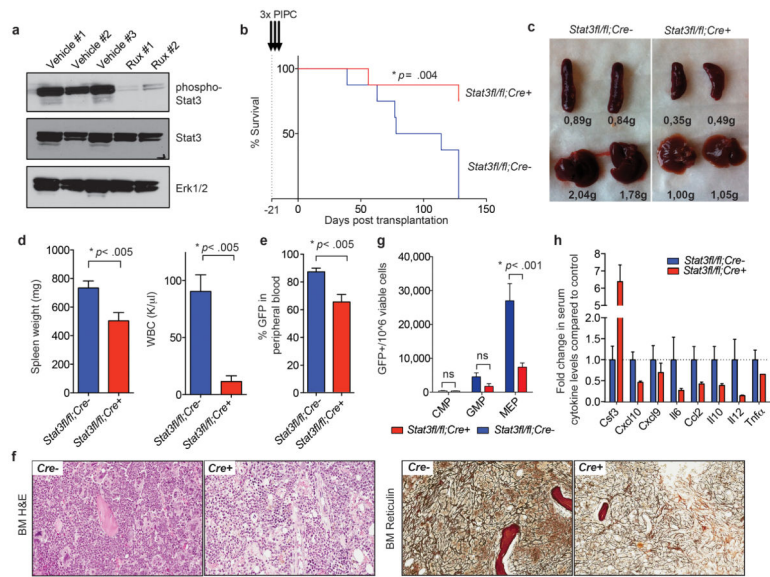


Figure 4. Deletion of *Stat3* reduces cytokine production and ameliorates MF *in vivo*
A, Western blot analysis of splenocytes from vehicle/ruxolitinib-treated MPLW515L diseased mice. **B–D** Deletion of *Stat3* prolongs survival (**B**, $n=8$) and reduces organomegaly (**C**) and leukocytosis (**D**) in the MPLW515L BMT model compared to control mice. Mean \pm s.e.m. of two independent experiments. **E**, Peripheral blood flow cytometric analysis. **F**, Reduced bone marrow cellularity and reticulin fibrosis in the bone marrow of MPLW515L-expressing *Stat3^{fl/fl};Vav-Cre⁺* and MPLW515L-expressing *Stat3^{fl/fl};Vav-Cre⁻* mice. Representative pictures of three independent experiments. 20x magnification. **G**, Number of GFP-positive MEP cells is decreased in the bone marrow of mice transplanted with MPLW515L-expressing *Stat3*-deleted bone marrow compared to MPLW515L-diseased controls. Mean \pm s.e.m. of two independent experiments. *Vav-Cre⁺*: $n=16$, *Vav-Cre⁻*: $n=10$. **H**, *Stat3* deletion reduces serum cytokines in MPLW515L-transplanted recipient mice. *Vav-Cre⁺*: $n=10$, *Vav-Cre⁻*: $n=7$. Mean \pm s.e.m.

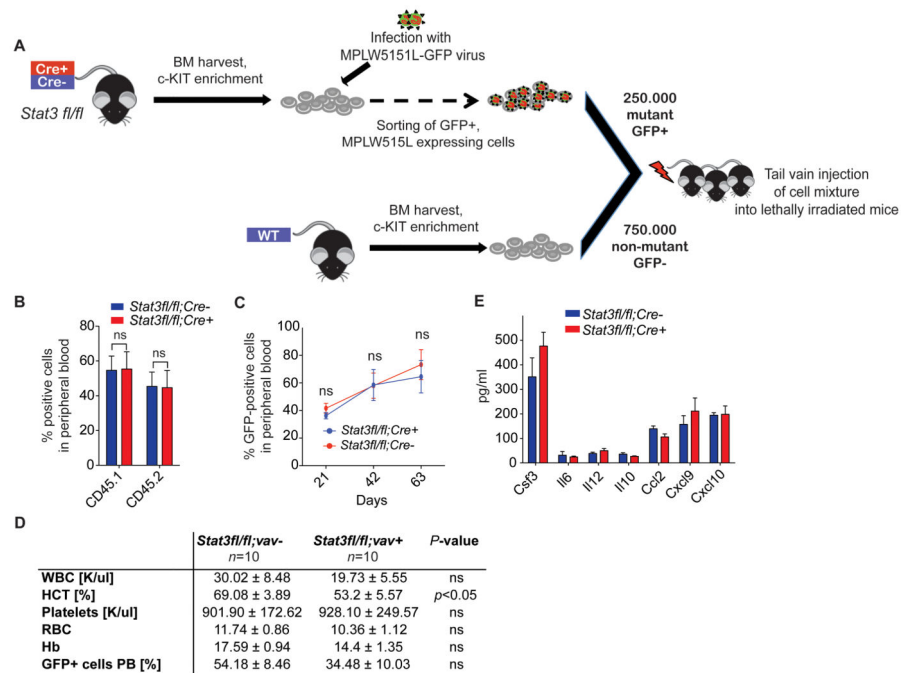


Figure 5. Mutant-restricted deletion of *Stat3* does not affect disease severity *in vivo*

A, Schematic illustration of bone marrow transplantation experiments using *Stat3*-deficient mice or littermate control mice as donors. Bone marrow cells were harvested from *Stat3* knock-out or wild-type control littermates, infected with MSCV-*hMPLW515L*-IRES-GFP and sorted for GFP. 250,000 GFP-positive cells were injected with 750,000 wild-type support marrow into lethally irradiated, wild-type (CD45.1) recipient mice. **B**, Depiction of peripheral blood chimerism of CD45.1-positive recipient mice transplanted with sorted CD45.2-positive MPLW515L-expressing; *Stat3^{fl/fl}; Vav-Cre^{+/-}* cells and CD45.1 support (d14 post transplantation). **C**, Deletion of *Stat3* in the mutant compartment does not reduce the proportion of GFP-positive cells in the peripheral blood, $n=10$ /group of which 4 were sacrificed at day 48 for analysis. **D**, Elevated cytokine levels with mutant-specific *Stat3* deletion. **E**, Differential blood counts of diseased mice which were transplanted with *Stat3^{fl/fl}; Cre-Vav⁺* or *Stat3^{fl/fl}; Cre-Vav⁻* MPLW515L transduced cells with 500,000 wild-type support marrow. $n=10$ /group.

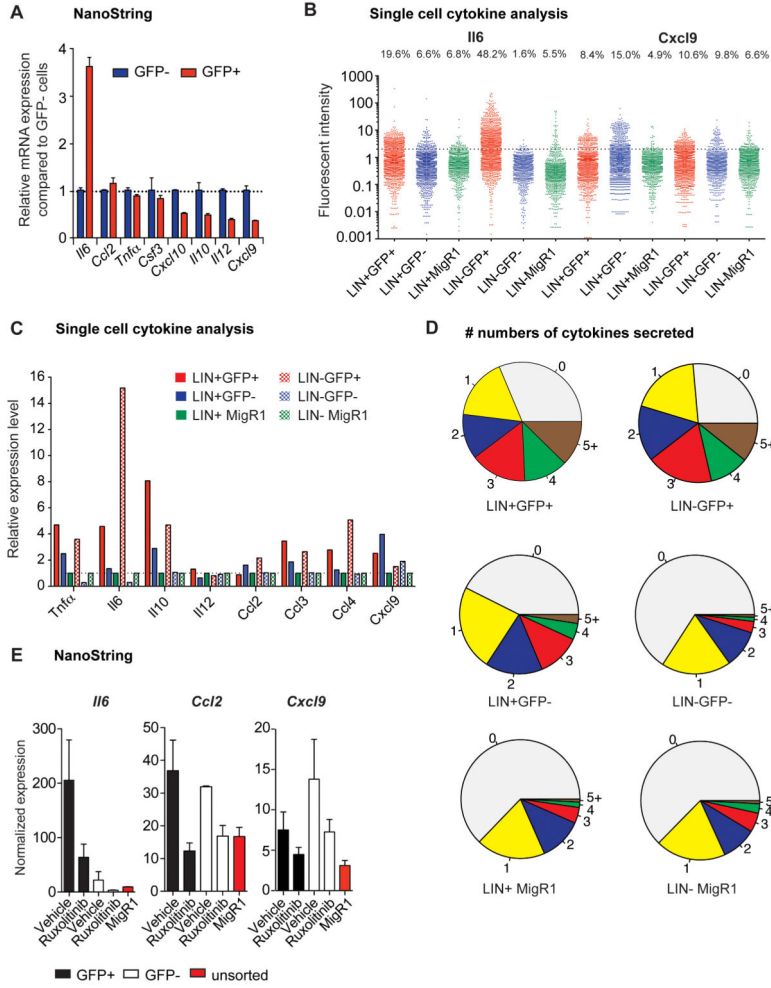


Figure 6. Pro-inflammatory cytokines are derived from malignant and non-malignant hematopoietic cells
A, NanoString mRNA cytokine expression levels in GFP-positive (GFP+) and GFP-negative (GFP-) cells. Normalized expression values calculated as relative change compared to GFP-negative cells. Results of one of two replicate experiments are displayed. **B**, Single cell cytokine analysis of sorted populations showing fluorescent intensity. MigR1-expressing bone marrow was used as control. Percentages of cytokine secreting cells are shown above. Dashed line indicates normalized cytokine secretion threshold. **C**, Cytokine expression of sorted GFP-positive/GFP-negative lineage-positive (LIN+) and lineage-negative (LIN-) cells of MPLW515L-diseased mice relative to MigR1 control bone marrow. **D**, Pie charts depicting percentage of sorted GFP-negative/positive lineage-positive/negative MF cells and MigR1 control cells secreting different numbers of cytokines. Numbers in brackets represent the percentage of cells secreting a given number of cytokines. **E**, NanoString expression data (mean ± s.e.m.) for lineage-positive GFP-positive and GFP-negative cells from vehicle/ruxolitinib-treated MPLW515L-diseased mice. Data from MigR1 transplanted mice are shown as control. *n*=3/group.

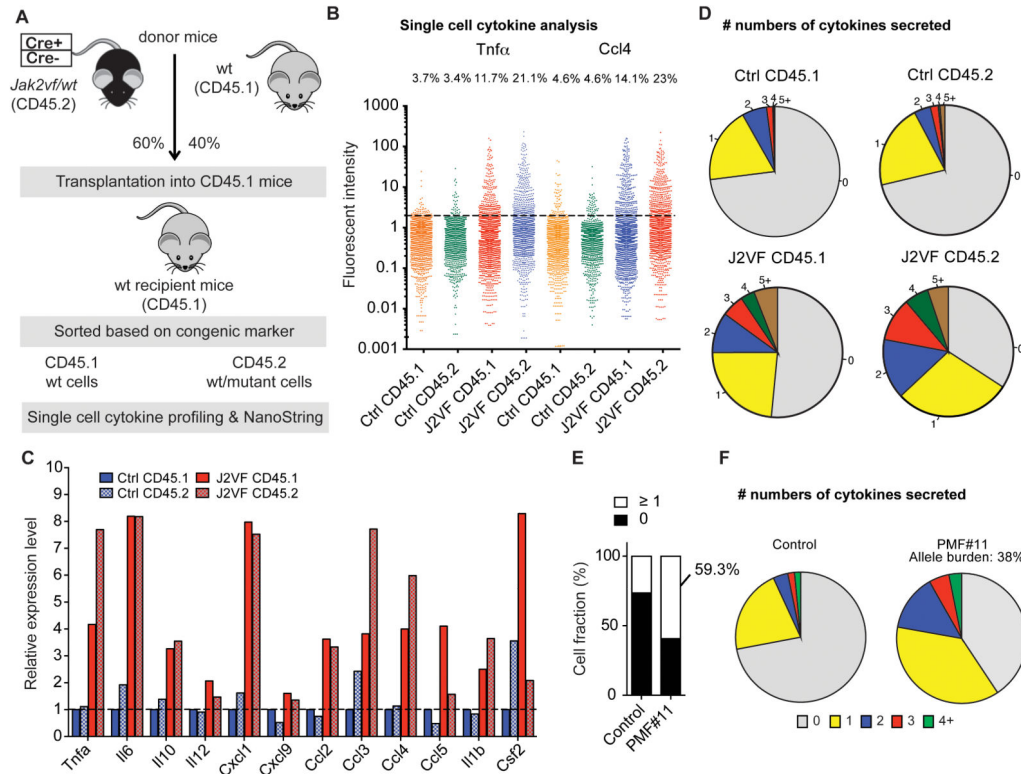


Figure 7. Aberrant cytokine production in CD45.2 mutant and CD45.1 non-mutant cells from JAK2V617F-diseased mice

A, Schematic illustration of bone marrow transplantation experiments using *Jak2V617F*;*Vav-Cre* knock-in mice (CD45.2) as donors. **B**, Single cell analysis of sorted mutant (CD45.2) and non-mutant (CD45.1) populations from *Jak2V617F*-diseased mice (J2VF) and transplanted healthy controls (Ctrl). Percentages of cytokine secreting cells are shown above. **C**, Cytokine expression levels of sorted CD45.1-positive and -negative MF and *Vav-Cre*-negative control cells relative to CD45.1 control cells. **D**, Pie charts displaying the percentage of sorted mutant (CD45.2) and non-mutant (CD45.1) secreting different numbers of cytokines (0,1,2,3,4,5+). **E**, Cytokine secretion data showing that 59.3% of human PMF cells (patient PMF#11, allele burden: 38%) secrete at least one cytokine. **F**, Pie charts depicting the percentage of human PMF cells and control cells secreting different numbers of cytokines (0,1,2,3,4+).